Mud depocentres on the continental shelf: a neglected sink for anthropogenic contaminants from the coastal zone

Michel Michaelovitch de Mahiques[1], Till J. J. Hanebuth[2], César C. Martins[3], Isabel Montoya-Montes[1], Javier Alcántara-Carrio, Rubens C. L. Figueira[1], Marcia C. Bícego[1]

[1] Instituto Oceanográfico da Universidade de São Paulo, Praça do Oceanográfico, 191, São Paulo, SP 05508-120, Brazil

[2] School of Coastal and Marine Systems Science, Coastal Carolina University, P.O. Box 261954, Conway, SC 29528, USA

[3] Centro de Estudos do Mar da Universidade Federal do Paraná, P.O. Box 61, Pontal do Paraná, PR 83255-976, Brazil

Abstract

In this study, published and unpublished data from the Santos Estuarine Complex and Bay and the adjacent continental shelf (São Paulo State, Brazil) were gathered in order to evaluate the entrapment of anthropogenic chemical contaminants (hydrocarbons, heavy metals) in a mid-shelf mud depocentre. Results show that these contaminants, produced by industrial activities in the adjacent coastal zone and released into the bay waters, are distributed far over the shelf since they are found in the mid-shelf mudbelt in locally significant concentrations. Two main aspects are highlighted by this study. The first underlines the fact that the material stored in the mudbelt is not related to a specific fluvial source discharging to the shelf. Instead, the contaminants, used as tracers, stem from multiple injection sources along the heavily used coastline of the Santos industrial zone. The second finding suggests that the anthropogenic compounds are not only accumulating in the surface sediments of fine-grained shelf depocentres. Rather, these substances are also already found several centimetres below the modern seabed. They can, thus, be easily reinjected into the water column by storms, benthic activity, and human disturbances such as seabed dredging and bottom trawling.

Keywords: Mudbelt. Continental shelf. Polycyclic aromatic hydrocarbons. Metals.
Shelf sedimentation. Source to sink

INTRODUCTION

The continental shelf is a complex system in which seabed morphology, subbottom stratigraphy, sedimentary surface processes, benthic ecology, and human-related modifications interact in a complex environment where wind-driven waves, tides, ocean currents, material input from the continent, and human activity find an imprint through time and space (Nittrouer et al. 2007; Shi et al. 2012). Among numerous reasons which make continental shelves relevant to human societies, one might highlight that shelves (a) are the most proximal and sensitive marine environments in the land-to-sea system;
(b) contain significant scarce resources of highest economic and ecological value;
(c) influence the impact of hazardous events on the coastal zone and its infrastructure; and (d) represent a potential sink for many kinds of anthropogenic substances, produced either offshore, in the coastal zone, or further inland.

The majority of modern clastic shelves are characterized by the presence of confined, elongated mud deposits which extend at a specific bathymetrical zone and which show individual three-dimensional geometries and sedimentary characteristics. The formation patterns result from the regional sea-level history and tectonic setting, the regional climate regime, type and intensity of river sediment input, and the regional to local shelf hydrodynamics, among other controlling factors (e.g. McCave 1972a; Edwards 2002; Gonsalez et al. 2004; McKee et al. 2004; Palinkas et al. 2006; Dubrulleet al. 2007; Sommerfield and Wheatcroft 2007; Lantzsch et al. 2009; Rose and Kuehl 2010; Oberle et al. 2014a).

The potential of these mudbelts as sinks for anthropogenic substances was reported by several studies for more than 20 years (e.g. Palanques et al. 1990, 2008; Lin and Chen 1996; Gonsalez et al. 2007; Hartwell 2008; Liu et al. 2011). The pathways of the transfer from the continental source to the proximal-marine sink are usually, but not necessarily, related to the existence of a dominant fluvial source (Lin et al. 2002; Palanques et al. 2008). Also, the anthropogenic contamination can be either of organic (Lee et al. 2006; Hartwell 2008) or of inorganic origin (Lin and Chen 1996; Ru´a et al. 2014). In this sense, sediment depocentres located at sites just off the coast show high concentrations of both organic and inorganic pollutants which are often affected by remobilization through human activities, e.g. bottom trawling fishing and dredging (Riemann and Hoffmann 1991; Warnken et al. 2003, Deepthi et al. 2014).

The south-eastern Brazilian shelf is adjacent to the most industrialized coastal area of Latin America, the Santos Estuarine Complex and Bay (SECB). The SECB houses one of the most important harbours in the Southern Hemisphere and an industrial complex with significant oil refining, petrochemical, and steel-producing industries. The area has a one-century history of organic and inorganic contamination which included intense water and air pollution, disposal of untreated sewage in the estuarine channels and mangrove fringes, and utilization of heavy metal-based antifouling ship paints. In fact, this situation started to change not earlier than in the early 1980s, when the government started a stricter control of environmental protection governance (Luiz-Silva et al. 2008;

Martins et al. 2010, 2011).

Moreover, apparently no major fluvial sources exist along this coast which could supply freshwater and terrigenous sediments to the shelf, since the drainage systems are rather limited in size due to the presence of a pronounced mountain chain along the coast (Serra do Mar). The maximum river flow which drains the area does not exceed 1000 $m^3 s^{-1}$ and is centred about 200 km to the south. Therefore, the distribution of the various anthropogenic substances to the adjacent shelf was for decades considered as being widely limited (Kowsmann et al. 1977). The possibility that any export of anthropogenic products to the shelf would find an imprint in the mid-shelf mud depocentres has, consequently, always been neglected. However, such an injection of contaminants to the ocean habitats at considerable levels would probably have severe ecological consequences.

The aim of this study is to characterize the continental shelf mud depocentres off the SECB as potential sinks for anthropogenic organic (particularly polycyclic aromatic hydrocarbons/PAHs and aliphatic hydrocarbons) and inorganic (heavy metals) components. The SECB continental shelf seafloor is located in close adjacency to the most industrialized area of South America and, thus, deserves a more detailed analysis on its role as a remote fate location of anthropogenic substances.

STUDY AREA

The Santos Estuarine Complex is a set of estuarine channels which receives the freshwater discharge of tens of small rivers originated in a coastal mountain chain (Serra do Mar) that is aligned with the SE Brazilian coast. Originally, this complex was fringed by exuberant mangrove forests that have been gradually substituted by the

Santos Harbour as well as by the most important steel and petrochemical complex of South America. The adjacent Santos Bay (Fig. 1, detail) is a 8.4-km-wide, 7.4-km-long embayment which receives the discharge of the main channels of the estuarine complex; it also corresponds to the only entrance of the Santos Harbour, the most active industrial port in Latin America (100.10^{6} tons in 2012).

The shelf off the SECB (Fig. 1) corresponds to the central part of the São Paulo Bight, an arc-shaped sector of the Brazilian inner continental margin, which extends from 22°Sto 28°S (Zembruscki 1979). The area in front of the SECB is characterized by a flat topography (1:1300) and very wide extent (230 km). The shelf-break occurs at about 160–180 mbsl (metres below modern sea level).

Due to the lack of a main fluvial input, the surface sediment distribution pattern is controlled by hydrodynamics and the local bathymetry (Mahiques et al. 2004). The inner shelf is covered by fine to very fine sands, extending down to the 50-m isobath. This sandy facies results from both wind-driven wave action and a northward-directed wind-driven shelf current, the latter being more effective during austral winter months.

The mid-shelf, extending from 50 to about 100 m, is characterized by the presence of several mudbelts in which the silty fraction prevails over the clays (Fig. 2; Mahiques et al. 2010). These sedimentary bodies are coast-parallel elongated, discontinuous in their lateral extent, and cover usually the palaeo-topography which was generated in the context of Late Pleistocene sea-level lowstands, e.g. times of long-lasting subaerial shelf exposure. The origin of the sediments filling these muddy depocentres is still a matter of debate. Mahiques et al. (2008) studied Nd and Pb isotopes in the shelf sediments located between 25°S and 27°S and showed mixed terrigenous source, with contributions from the remote (more than 1000 km) Rio de La Plata (basaltic rocks from the Paraná Basin) and a second yet undefined crustal source. This second source shows a well-marked Pb isotope signature from which the adjacent amphibolites, gneisses, and migmatites of the Serra do Mar mountain chain can at least not be discarded as potential source rocks. Sedimentation rates in this area vary from 13 to 33 cm kyr $^{-1}$ (Mahiques et al. 2011).

The outer shelf is characterized by a wide sheet of medium-to coarse-grained relict sands being result of the permanent floor-polishing effect of the meandering Brazil Current (Mahiques et al. 2002, 2004). In this outermost shelf zone, modern sedimentation rates are negligible and surface sediments date back to early Holocene ages (Mahiques et al. 2011).

The inner and mid-shelf hydrographical structure is determined by the seasonal displacement of three water masses with strong seasonal variation (Castro et al. 1987). Between November and March, the South Atlantic Central Water (SACW; T = 14.0 °C, S = 35.5) moves on the bottom towards the coast, leading to an oceanward displacement of the less dense superficial Coastal Water (CW; T = 22.0 °C, S \35.0) and keeping the outer-shelf Tropical Water (TW; T = 25.0 °C, S = 37.1) relatively distant from the coastline. This period corresponds to the rainy season in SE Brazil and, thus, to an increased terrigenous flux to the coastal waters. This superficial displacement of the CW is the most important factor in the transport of terrigenous organic matter towards the deeper areas of the shelf. From March to November, the retreat of the SACW leads to a greater influence of the TW on shelf processes (Mahiques et al. 1999).

MATERIALS AND METHODS

This paper gathers partially published (Figueira et al. 2006; Martins et al. 2007, 2008, 2010) and unpublished data from surface sediments and sediment cores (Fig. 1) collected in the Santos Estuarine Complex and Bay, as well as on the adjacent shelf, including a mid-shelf mudbelt depocentre.

For organic component analysis, eight sediment samples were collected in the Santos Bay while 21 samples were taken on the adjoining continental shelf at the sites shown in Fig. 1, using a box corer during the austral winter of 2005. The sediment surface layer (0–2 cm) was stored in pre-cleaned aluminium foil at -15 °C. Three of the box cores, taken in muddy areas, were continuously sampled in one-cm intervals. The sediments were freeze-dried, homogenized in a mortar, and stored in glass bottles until laboratory analysis.

Existing data for the SECB were in addition obtained from Martins et al. (2007, 2008, 2010).

The complete analytical protocol for PAH analysis is described in UNEP (1992). Around 20 g of sediment was extracted over 8 h by Soxhlet using 80 mL of a mixture of (1:1) dichloromethane (DCM) and n-hexane. Surrogates (naphthalene-d8, acenaphthene-d10, phenanthrene-d10, chrysene-d12, and perylene-d12) were added prior to sample extraction. The DCM/n-hexane extract was purified by column chromatography using 5 % deactivated alumina (1.8 g) and silica (3.2 g). The elution was done with 10 mL n-hexane (fraction 1—aliphatic hydrocarbons) and 15 mL (3:7) DCM/n-hexane mixture (fraction 2—PAHs). An aliquot of 1 µL from each extract was injected for gas chromatographic analysis.

The PAH analyses were performed with an Agilent GC model 6890 coupled to a Agilent Mass Spectrometer Detector (model 5973) and an Ultra-2 capillary fused silica column coated with 5 % diphenyl/dimethylsiloxane (30 m, 0.32 mm ID and 0.25 µm film thickness). The oven temperature was programmed to 40 °C holding for 2 min, to

40–60 °C with a temperature increase of 20 °C min^{-1}, then to 250 °C with 5 min^{-1}, and finally to 300 °C with 6 min^{-1}, where this temperature was always held for 5 min. Helium was used as the carrier gas, and the data acquisition was done in single-ion monitoring mode (SIM). The aliphatic hydrocarbons analyses were performed with an Agilent GC (model 6890) equipped with a flame ionization detector. The fused silica column and the temperature programme used to identify aliphatic hydrocarbons were identical to the procedure used for the quantification of PAHs.

Procedural blanks contained a few minor contaminant peaks, but these did not interfere with the analyses of target compounds. Detection limits (DL) for each PAH were approximately 0.50 ng g^{-1} dry weight. A surrogate and spiked-recovery experiment was conducted simultaneously with the extraction of the samples and the recovery ranged from 50 to 120 % (Martins et al. 2007, 2011). Measured concentrations of target PAHs and n-alkanes in the IAEA417 reference material were within 90 to 115 % of the certified values provided by the International Atomic Energy Agency (IAEA). Also, regular analyses of reference material (NIST 1941b) from the National Institute of Standards and Technology, USA, and annual participation in the inter-comparison exercises promoted by the Marine Environment Laboratory of International Atomic Energy Agency (MEL-IAEA) have shown satisfactory quality control.

Elemental analyses (Al, Sc, Cu, Pb, and Zn) were performed using the ICP-OES technique with a Varian model VISTA-MPX. The analysis followed the procedures described in Method 3050b of the SW-846 series (USEPA 2008). Approximately 1 g of dry sediment was digested with 10 mL of 1:1 HNO3 at 95 °C for 15 min. After cooling, another 5 mL of concentrated HNO3 was added, and the solution was heated for 30 min. This second procedure was repeated until the digestion of the sample was completed. 2 mL of water and 3 mL of 30 % H2O2 were added as the sample was heated until the elimination of the organic matter was completed.

After this step, 10 mL of concentrated HCl was added, and the solution was heated for 15 min. Finally, the solution was filtered through a Whatman 41 filter, and 10 mL of concentrated HCl was added to the digestate. Finally, the solution was filtered again with a Whatman 41 filter and the filtrate was collected in a 100-mL flask. The volume was filled up to 100 mL, and the solution was analysed in a Varian ICP-OES, model VISTA-MPX. The measurement precision for all elements was at least 5 %. Method accuracy was obtained by analysing certified standards of contaminated soils (SS-1 and SS-2 EnviroMAT).

Limits of detection and quantification as well as recovery percentage of the different metals are given in Table 1.

Table 1 Limits of detection and quantification as well as recovery percentage of the metal standards used in this study

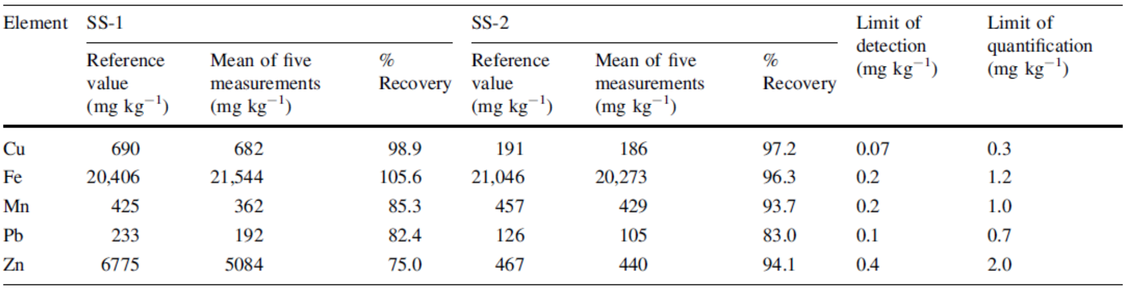

Element	SS-1			SS-2			Limit of detection (mg kg^{-1})	Limit of quantification (mg kg^{-1})
	Reference value (mg kg^{-1})	Mean of five measurements (mg kg^{-1})	% Recovery	Reference value (mg kg^{-1})	Mean of five measurements (mg kg^{-1})	% Recovery		
Cu	690	682	98.9	191	186	97.2	0.07	0.3
Fe	20,406	21,544	105.6	21,046	20,273	96.3	0.2	1.2
Mn	425	362	85.3	457	429	93.7	0.2	1.0
Pb	233	192	82.4	126	105	83.0	0.1	0.7
Zn	6775	5084	75.0	467	440	94.1	0.4	2.0

RESULTS AND INITIAL INTERPRETATION

Tables 2 and 3 summarize the results obtained for the three different sedimentary environments considered here: Santos Estuarine Complex, Santos Bay and the on the adjoining shelf. Figures 3 and 4 present the box plots of the anthropogenic compounds in the different environments and the bathymetrical behaviour of the same compounds, respectively. Figure 5 (a to d) presents the geographical distribution of metals and organic constituents in the surface sediments on the continental shelf.

Trace metals in surface and subsurface sediments of the SECB and adjacent continental shelf

Inside the Santos Estuarine Complex, the values of lead (Pb) concentrations varied from 9 mg kg $^{-1}$ (pre-industrialized, non-contaminated sediments) to 59 mg kg $^{-1}$ (top core samples from the harbour). Concerning zinc (Zn), the values ranged from 54 to 128 mg kg $^{-1}$ (same samples as for Pb).

Surface sediments of Santos Bay showed a variation in the same order of magnitude as for Pb (N.D., i.e. below the limit of detection to 38 mg kg $^{-1}$), but at least one significantly higher value for Zn (range from 9 to 274 mg kg $^{-1}$). As for the organic compounds, the spatial variance of heavy metals in the sediments of Santos Bay is much higher than in the other two environments.

Finally, sediments collected on the shelf off the SECB exhibit values ranging from 2 to 11 mg kg $^{-1}$ for Pb and 6 to 50 mg kg $^{-1}$ for Zn (Figs. 4, 5).

Elemental copper occurs in small concentrations in the three environments (maximum of 48 mg kg $^{-1}$ in the cores from the Estuarine Complex, 38 mg kg $^{-1}$ in the Santos Bay samples, and 10 mg kg $^{-1}$ in the shelf sediments).

The observation of the bathymetrical behaviour for both organic compounds and the trace metals (Figs. 4, 5, 6) shows a clear gap between the isobaths at approximately 30–90 m. In fact, this zone isolates two of the mudbelts present on the shelf, one located close to the coast and the second on the middle shelf.

It is noticeable that the metal concentrations in samples from the Estuarine Complex and Santos Bay exceeded the Interim Sediment Quality Guidelines (ISQG) and even the Probable Effect Levels (PEL) for Cu, Pb, and especially Zn (available at http://st-ts.ccme.ca/en/index.html).

Organic compounds in surface and subsurface sediments of the SECB and the adjacent continental shelf

Inside the Santos Estuarine Complex, the ΣPAH concentrations in the core sediments varied greatly, ranging from 3.3 ng g^{-1} in basal, i.e. pre-industrial layers to 7987.1 ng g^{-1} at highly contaminated places.

In the Santos Bay, the ΣPAH concentration of surface sediments varied from N.D. to 319.1 ng g^{-1}, with a mean concentration of 158.5 ± 103.5 ng g^{-1}(n = 6). The highest concentrations (319.1 ng g^{-1}) were found in the proximity to a sewage outfall, as well as close to the main entrance of Santos Harbour (227.5 ng g^{-1}).

Table 2 Synthesis of the concentrations of polycyclic aromatic hydrocarbons (PAHs), aliphatic hydrocarbons, and metals in the studied environments

	Sector																			
	Estuary																			
	Core SR				Core CS1				Core CS2				Core CN				Core BER			
	Mean	SD	Max	Min	Mean	SD	Max	Min	Mean	SD	Max	Min	Mean	SD	Max	Min	Mean	SD	Max	Min
ΣPAH (ng $g^{N.A.1}$)	2301.3	1335.3	3809.7	50.5	2390.6	2151.8	7987.1	< d.l.	192.7	481.7	2108.7	3.2	157.3	183.7	721.6	15.5	N.A.	N.A.	N.A.	N.A.
Σ Aliphatic (μg $g^{N.A.1}$)	198.3	152.6	464.2	3.9	296.6	225.7	667.8	10.9	12.4	3.6	21.0	8.9	13.0	6.5	32.2	2.9	N.A.	N.A.	N.A.	N.A.
Pb (mg $kg^{N.A.1}$)	34	5	42	25	41	7	59	30	N.A.	N.A.	N.A.	N.A.	N.A.	N.A.	N.A.	N.A.	12	2	15	9
Cu (mg $kg^{N.A.1}$)	20	12	24	16	24	8	48	16	N.A.	N.A.	N.A.	N.A.	N.A.	N.A.	N.A.	N.A.	6	1	7	4
Fe (mg $kg^{N.A.1}$)	3171	216	3500	2900	3638	260	4100	3200	N.A.	N.A.	N.A.	N.A.	N.A.	N.A.	N.A.	N.A.	2892	150	3100	2600
Mn (mg $kg^{N.A.1}$)	N.A.	N.A.	N.A.	N.A.	N.A.	N.A.	N.A.	N.A.	N.A.	N.A.	N.A.	N.A.	N.A.	N.A.	N.A.	N.A.	N.A.	N.A.	N.A.	N.A.
Zn (mg $kg^{N.A.1}$)	99	6	108	83	93	20	128	70	N.A.	N.A.	N.A.	N.A.	N.A.	N.A.	N.A.	N.A.	65	6	75	54

	Sector							
	Santos Bay				Shelf			
	Mean	SD	Max	Min	Mean	SD	Max	Min
ΣPAH (ng $g^{N.A.1}$)	158.5	103.5	319.1	18.5	83.1	58.3	147.3	6.7
Σ Aliphatic (μg $g^{N.A.1}$)	8.4	10.5	23.0	0.3	1.7	1.8	6.4	0.7
Pb (mg $kg^{N.A.1}$)	17	8	38	N.D.	5	2	11	2
Cu (mg $kg^{N.A.1}$)	11	1	38	4	2	3	10	N.D.
Fe (mg $kg^{N.A.1}$)	20513	7465	41600	11100	7211	5089	21829	2532
Mn (mg $kg^{N.A.1}$)	343	213	873	54	216	301	1240	32
Zn (mg $kg^{N.A.1}$)	47	43	274	9	16	11	50	6

"N.A." refers to samples having Not been Analysed and "N.D." to concentrations below the limit of detection

Table 3 Down-core concentration profiles of polycyclic aromatic hydrocarbons (PAHs) and aliphatic hydrocarbons in the three box cores discussed

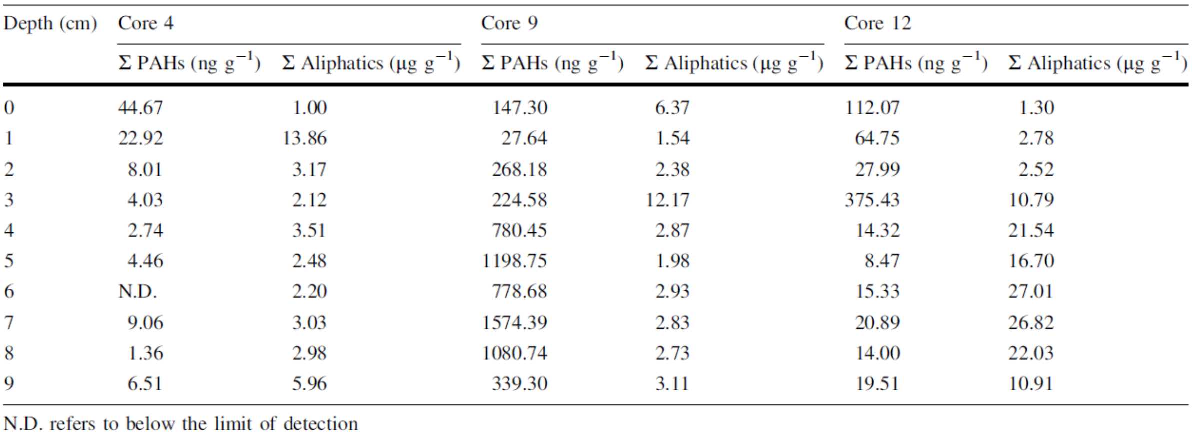

Depth (cm)	Core 4		Core 9		Core 12	
	Σ PAHs (ng g^{-1})	Σ Aliphatics (μg g^{-1})	Σ PAHs (ng g^{-1})	Σ Aliphatics (μg g^{-1})	Σ PAHs (ng g^{-1})	Σ Aliphatics (μg g^{-1})
0	44.67	1.00	147.30	6.37	112.07	1.30
1	22.92	13.86	27.64	1.54	64.75	2.78
2	8.01	3.17	268.18	2.38	27.99	2.52
3	4.03	2.12	224.58	12.17	375.43	10.79
4	2.74	3.51	780.45	2.87	14.32	21.54
5	4.46	2.48	1198.75	1.98	8.47	16.70
6	N.D.	2.20	778.68	2.93	15.33	27.01
7	9.06	3.03	1574.39	2.83	20.89	26.82
8	1.36	2.98	1080.74	2.73	14.00	22.03
9	6.51	5.96	339.30	3.11	19.51	10.91

N.D. refers to below the limit of detection

The ΣPAH concentrations in surface sediments on the adjoining continental shelf varied from N.D. to 147.3 ng g $^{-1}$, with a mean concentration 83.07 (n = 4). PAH concentrations were detected only at Stations 7, 9, 12, and 21. Stations 7 and 9 (66.4 and 147.3 ng g $^{-1}$, respectively) are those located close to an area at the exit of Santos Bay, which is used as disposal area of the sediments dredged in the SECB. Sites 12 and 21 (112.1 and 6.65 ng g $^{-1}$, respectively) are located in a mid-shelf mudbelt at the 100-m isobath (Fig. 6).

In the estuarine sediments, the concentrations of the total aliphatic hydrocarbons (ΣAliph) exhibit clear differences among the sediment cores. Two of the cores show very high ΣAliph concentrations (maxima of 464.2 and 667.8 µgg $^{-1}$) while two others have maxima of 21.0 and 32.2 µgg $^{-1}$, giving the spatial deposition of these organic compounds along the estuarine system a local character.

Surface sediments from Santos Bay show values which are coherent with the less contaminated sediments from the estuarine cores, with a ΣAliph average value of -1 -1

8.4 ± 10.5 μgg , ranging from 0.33 to 22.97 μgg (n = 8). Worth noting is the high dispersion of the ΣAliph values which, in fact, follows the grain size variations in the area (Fukumoto et al. 2004).

Surface sediments from the adjacent shelf show a pattern of low ΣAliph values, ranging from 0.7 to 6.4 μgg^{-1} (average 1.68 ± 1.42 μgg^{-1}), with the highest values located in the mid-shelf mudbelt.

Organic compounds in box cores

The analysis of the vertical distribution of the organic compounds along the box cores (Fig. 7) collected on the shelf revealed that the highest values are not located at the shallowest, e.g. youngest layer. On the contrary, both ΣPAH and ΣAliph show a vertical variation in which deeper layers can reach two orders of magnitude higher values than the uppermost layer does. This is particularly the case for one of the samples (#12) collected on the midshelf mudbelt which shows values of 375.4 ng g^{-1} of ΣPAH and 12.2 μgg^{-1} of ΣAliph at 4 cm sediment depth. It is worth noting that these elevated values in the mudbelt appear in the same order of magnitude as those measured on the directly contaminated muds from the Santos Bay.

A second core also collected from the mid-shelf mudbelt showed detectable concentrations of PAHs and aliphatic hydrocarbons throughout its whole sedimentary succession.

A third core (#9) was collected at the disposal site of dredged materials of the Santos Channel and, thus, presents values as high as 1,574.0 ng g^{-1} of ΣPAH and 27.0 μgg^{-1} of ΣAliph. In this core, the concentrations have drastically increased between 9 and 7 cm and gradually decreased to lower values since then.

DISCUSSION

Given the absence of bioturbation as indicated by a millimetre-scale laminated texture found in the sediment cores of the mid-shelf mudbelt off Santos, as also verified by macroscopic analysis, two observations are noticeable: the deposition of the organic compounds in the mid-shelf mudbelt reaches locally significant levels of contamination on the one hand, and did not accumulate at constant rates through time and not in equal spatial distribution on the other. This observation might be related to one of the following two processes: (a) Lateral variations in local sedimentation rates or in local shelf hydrodynamics led to a differentiated distribution pattern of particulate contaminant-absorbing matter. Shelf dynamics and local sources of sediment lead to the generation of a full mosaic of sediment types and (b) Production and injection of anthropogenic compounds have changed through time (Martins et al. 2007). Given the comparably low values measured in the uppermost centimetres, this second scenario might be related to the stricter policy for pollution control since the 1980s (Luiz-Silva et al. 2008).

While the contamination of sediments in estuaries and bays is demonstrated for many systems (Cearreta et al. 2013; Gao et al. 2013), the fact that these pollutants are also stored at significant concentrations in open-shelf mudbelts is yet little documented (e.g. McKee et al. 2004).

The laterally offshore spreading of the riverine suspension tongue distributing the contaminants from the coastal zone towards the inner and middle continental shelf might be driven by one of the following hydrodynamic processes.

a) Seasonally enhanced fluvial run-off as a result of heavy precipitation events often leads to peaks in suspension load (e.g. Summerfield and Nittrouer 1999; Geyer et al. 2004). This plume would then spread out allowing the particles to rain down in the open-shelf waters, as stated by Mahiques et al. (1999) for the studied area;

b) Bottom waters enriched in sediment suspension tend to be offshore advected by gravity, thus flowing down the comparably steep shoreface to inner-shelf gradient towards the mid-shelf zone (e.g. McCave 1972; Traykovski et al. 2000). The high bottom sediment concentration might be the result of an early freshwater-plume/suspension-plume separation after being supplied into the ocean (e.g. Hill et al. 2007; Geyer et al. 2004; McKee et al. 2004), or of intense remobilization of fine-grained inner-shelf seabed sediments by storm events; (c) An alternative mechanism for offshore transport of suspended matter is the wind-driven normal-to-coast circulation of coastal waters (Vitorino et al. 2002; Geyer et al. 2004). Such a local downwelling scenario enhances the gravity-driven offshore motion of the bottom layer (see b) and injects additional fines to the bottom turbidity layer.

With increasing distance to the coast, the river-and wind-driven surface influences become less effective and the seabed shows a gentler gradient. Thus, the inner boundary of the mid-shelf mud depocentres is commonly controlled by the vertical limit of the storm weather wave base combined with the decrease in the efficiency of gravity forcing (e.g. McCave 1972; Jouanneau et al. 2002).

These mud depocentres represent a major sink for fine-grained continent-derived materials and form in a water-depth interval of calm hydrodynamic conditions (e.g. McCave 1972; Walsh and Nittrouer 2009). Since most of these deposits develop since several millennia (e.g. Hanebuth et al. 2015), the contaminants should be assumed as being retained for long times. These mud depocentres serve as cradle for benthic life on lower and higher tropic levels of the food chain, including fish larvae (e.g. Thrush and Dayton 2002). It should, thus, be expected that these organisms accumulate these contaminants in significant amounts. When they incorporated them into their fabric, they do not only recycle these substances, but also inject them back into the water column or into the food chain, respectively. In addition and in some regions of high relevance, the disturbance of these mud deposits by recently changing regional climatic conditions (for instance, increase in high-energy storm events; e.g. Pezza and Simmonds 2005; McTaggart-Cowan et al. 2006; George and Hill 2008) or by chronic human seabed activity (material dredging, bottom trawling fishery; e.g. Pilskaln et al. 1998; Torres et al. 2009) probably leads to a progressive release of these contaminants into the water column at severe levels.

Studies have further shown that significant amounts of suspended muds which were originally introduced to the shelf system by the regional rivers are not stored on the shelf itself but are transported towards the open, i.e. deep ocean (e.g. Nittrouer et al. 2007; Oberle et al. 2014b). Accepting these general bypassing and seasonal remobilization processes of the particulate suspended matter as being relevant, a long-distance offshore distribution of these contaminants and its ecological impact is probably much severe than yet expected.

CONCLUSIONS

Despite the absence of direct river input to the continental shelf, an export process of anthropogenic materials exists in the study area being responsible for the offshore transport of contaminants in measureable and partly significant amounts, which finally deposit in mudbelts located on the mid-shelf off SE Brazil. This coastal material distribution process might be linked to seasonal flood-like run-off after heavy rain events, to gravity-driven advection of suspension-rich bottom waters or to wind-driven vertical, normal-to-coast circulation of coastal waters. The only potential source of these anthropogenic materials is the metropolitan zone of Santos Harbour, the largest port in South America.

This study shows that industry-related contamination in coastal regions is not solely restricted to the immediate coastal zone, comprising river mouth and estuarine environments. Rather, these contaminants are widely distributed over the adjacent continental shelf and might be available for recycling processes for an unestimated long time.

The observed elevated concentrations of anthropogenic substances in deeper, i.e., older stratigraphic layers of the mudbelt deposit indicate that either input or accumulation was not constant trough time. Bioturbation or physical vertical material mixing can be excluded as being responsible for a downward transport in the sediment column because the sediments are finely laminated and the values in deeper strata are, also, sometimes even higher than those measured at the sediment surface. Changes in the hydrodynamic system or in the production of the contaminants might be actual scenarios to explain the heterogeneous distribution pattern found in the mud depocentre. To prove these potential relations (local internal control; industrial production history; climate variability) will be a future task.

Acknowledgments. This article is related to the project entitled ‘‘A Influência do Complexo Estuarino da Baixada Santista sobre o Ecossistema da Plataforma Adjacente—ECOSAN’’ sponsored by FAPESP (Grant No. 03/09932-1). FAPESP also supported grant 10/06147-5 for the acquisition of R.V. Alpha Crucis which allowed the obtainance of chirp subbottom echo sounder data. Acknowledgement is due to K. Lindhorst, University of Kiel, who kindly processed the chirp profile shown in Fig. 2. The authors would also like to express their gratitude to the crews of the B.Pq. Velliger II and the R.V. Prof. W. Besnard for the collection of samples. Michel Mahiques acknowledges the Brazilian National Research Council (CNPq) for Research Grant No. 301106/2010-0. This publication is related to the INQUA International Focus Group ‘‘Rapid environmental changes and human impact on continental shelves’’.

REFERENCES

Castro BM, Miranda LB, Miyao SY (1987) Condições hidrográficas na plataforma continental ao largo de Ubatuba: variações sazonais e em média escala. Bol Inst Oceanogr 35:135–151

Cearreta A, García-Artola A, Leorri E, Irabien MJ, Masque P (2013) Recent environmental evolution of regenerated salt marshes in the southern Bay of Biscay: anthropogenic evidences in their sedimentary record. J Mar Syst 109–110: S203–S212

Deepthi K, Natesan U, Muthulakshmi AL, Ferrer VA, Venugopalan VP, Narasimhan SV (2014) Heavy metals in nearshore sediments of Kalpakkam, southeast coast of India. Environ Earth Sci 72:717–729

Dubrulle C, Jouanneau JM, Lesueur P, Bourillet JF, Weber O (2007) Nature and rates of fine-sedimentation on a mid-shelf: ‘‘La Grande Vasière’’ (Bay of Biscay, France). Cont Shelf Res 27:2099–2115

Edwards BD (2002) Variations in sediment texture on the northern Monterey Bay

National Marine Sanctuary continental shelf. Mar Geol 181:83–100

Figueira RCL, Tessler MG, Mahiques MM, Cunha IIL (2006) Distribution of Cs-137, Pu-238 and Pu239 + 240 in sediments of the southeastern Brazilian shelf—SW Atlantic margin. Sci Total Environ 357:146–159

Fukumoto MM, Mahiques MM, Tessler MG (2004) Bottom faciology and sediment transport in Santos Bay, Southeastern Brazil. J Coast Res 39:1737–1740

Gao Y, de Brauwere A, Elskens M, Croes K, Baeyeens W, Leermakers M (2013) Evolution of trace metal and organic pollutant concentrations in the Scheldt River Basin and the Belgian Coastal Zone over the last three decades. J Mar Syst 128:52–61

George DA, Hill PS (2008) Wave climate, sediment supply and the depth of the sand–mud transition: a global survey. Mar Geol 254:121–128

Geyer WR, Hill PS, Kineke GC (2004) The transport, transformation and dispersal of sediment by buoyant coastal flows. Cont Shelf Res 24:927–949

Gonsalez R, Dias JMA, Lobo F, Mendes I (2004) Sedimentological and paleoenvironmental characterisation of transgressive sediments on the Guadiana Shelf (Northern Gulf of Cadiz, SW Iberia). Quat Int 120:133–144

Gonsalez R, Araujo MF, Burdloff D, Cachão M, Cascalho J, Corredeira C, Dias JMA, Fradique C, Ferreira J, Gomes C, Machado A, Mendes I, Rocha F (2007) Sediment and pollutant transport in the Northen Gulf of Cadiz: a multi-proxy approach. J Mar Syst 68:1–23

Hartwell SI (2008) Distribution of DDT and other persistent organic contaminants in canyons and on the continental shelf off the central California coast. Mar Environ Res 65:199–217

Hill PS, Fox JM, Crockett JS, Curran KJ, Friedrichs CT, Geyer WR, Milligan TG, Ogston AS, Puig P, Scully ME, Traykovski PA, Wheatcroft RA (2007) Sediment delivery to the seabed on continental margins. In: Nittrouer CA, Austin JA, Field ME, Kravitz JH, Syvitski JPM, Wiberg PL (eds) Continental margin sedimentation: from sediment transport to sequence stratigraphy. Special Publication of the International Association of Sedimentologists, no 37. Blackwell, Malden, pp 49–99

Jouanneau JM, Weber O, Drago T, Rodrigues A, Oliveira A, Dias JMA, Garcia C, Schmidt S, Reyss JL (2002) Recent sedimentation and sedimentary budgets on the western Iberian shelf. Prog Oceanogr 52:261–275

Kowsmann RO, Costa MPA, Vicalvi MA, Coutinho MGM, Gamboa LAP (1977) Modelo da sedimentação holocênica na plataforma continental sul brasileira. In: Projeto REMAC—Evolução sedimentar holocênica da plataforma continental e do talude do Sul do Brasil. Se´rie Projeto REMAC. Petrobrás, Rio de Janeiro, vol 2, pp 7–26

Lantzsch H, Hanebuth TJJ, Bender V (2009) Holocene evolution of mud depocentres on a high-energy, low accumulation shelf (NW Iberia). Quat Res 72:325–336

Lee CM, Lin TY, Lin CC, Kohbodi GA, Bhatt A, Lee R, Jay JA (2006) Persistence of fecal indicator bacteria in Santa Monica Bay beach. Water Res 40:2593–2602

Lin S, Chen CM (1996) Spatial variations of heavy metals in the east China Sea continental shelf surface sediments. Chem Ecol 13:77–91

Lin S, Hsieh IJ, Huang KM, Wang CH (2002) Influence of the Yangtze River and grain size on the spatial variations of heavy metals and organic carbon in the East China Sea continental shelf sediments. Chem Geol 182:377–394

Liu S, Shi S, Zhu Z, Yang G, Zhu A, Gao J (2011) Concentration distribution and assessment of heavy metals in sediments of mud area from inner continental shelf of the East China Sea. Environ Earth Sci 64:567–579

Luiz-Silva W, Machado W, Matos RHR (2008) Multi-elemental contamination and historic record in sediments from the Santos-Cubatão Estuarine System, Brazil. J Braz Chem Soc 19:1490–1500

Mahiques MM, Mishima Y, Rodrigues M (1999) Characteristics of the sedimentary organic matter on the inner and middle continental shelf between Guanabara Bay and São Francisco do Sul, Southeastern Brazilian Margin. Cont Shelf Res 19:775–798

Mahiques MM, Silveira ICA, Sousa SHM, Rodrigues M (2002) Post-LGM sedimentation on the outer shelf/upper slope in the northernmost part of the São Paulo Bight, South-Eastern Brazil. Mar Geol 181:387–400

Mahiques MM, Tessler MG, Ciotti AM, Silveira ICA, Sousa SHM, Figueira RCL, Tassinari CCG, Furtado VV, Passos RF (2004) Hydrodynamically-driven patterns of recent sedimentation in the shelf and upper slope off southeast Brazil. Cont Shelf Res 24:1685–1697

Mahiques MM, Tassinari CCG, Marcolini S, Violante R, Figueira RCL, Silveira ICA, Sousa SHM (2008) Nd and Pb isotope signatures on the Southeastern South American Upper Margin: implications for sediment transport and source rocks. Mar Geol 250:51–63

Mahiques MM, Sousa SHM, Furtado VV, Tessler MG, Toledo FAL, Burone L, Figueira RCL, Klein DA, Martins CC, Alves DPV (2010) The Southern Brazilian shelf: general characteristics, sediment distribution and Quaternary evolution. Braz J Oceanogr 58:25–34

Mahiques MM, Sousa SHM, Burone L, Nagai RH, Silveira ICA, Figueira RCL, Soutelino RG, Ponsoni L, Klein DA (2011) Radiocarbon geochronology of the sediments of the São Paulo Bight (southern Brazilian upper margin). An Acad Bras Cienc 83:817–834

Martins CC, Mahiques MM, Bícego MC, Fukumoto MM, Montone RC (2007) Comparison between anthropogenic hydrocarbons and magnetic susceptibility in sediment cores from the Santos Estuary, Brazil. Mar Pollut Bull 54:240–246

Martins CC, Ferreira JA, Taniguchi S, Mahiques MM, Bícego MC, Montone RC (2008) Spatial distribution of sedimentary linear alkylbenzenes and faecal steroids of Santos Bay and adjoining continental shelf, SW Atlantic, Brazil: origin and fate of sewage contamination in the shallow coastal environment. Mar Pollut Bull 56:1359–1363

Martins CC, Bícego MC, Mahiques MM, Figueira RCL, Tessler MG, Montone RC (2010) Depositional history of sedimentar linear alkylbenzenes (LABs) in a large South American industrial coastal area (Santos Estuary, Southeastern Brazil). Environ Pollut 158:3355–3364

Martins CC, Bícego MC, Mahiques MM, Figueira RCL, Tessler MG, Montone RC (2011) Polycyclic aromatic hydrocarbons (PAHs) in a large South American industrial coastal area (Santos Estuary, Southeastern Brazil): sources and depositional history. Mar Pollut Bull 63:452–458

McCave IN (1972) Transport and escape of fine-grained sediment from shelf areas. In: Swift DJP, Duane DB, Pilkey O (eds) Shelf sediment transport: process and pattern. Dowden, Hutchinson and Ross Eds, Stroudsburg, pp 225–244

McKee BA, Aller RC, Allison MA, Bianchi TS, Kineke GC (2004) Transport and transformation of dissolved and particulate materials on continental margins influenced by major rivers: benthic boundary layer and seabed processes. Cont Shelf Res 24:899–926

McTaggart-Cowan R, Bosart LF, Davis CA, Atallah EH, Gyakum JR, Emanuel KA (2006) Analysis of Hurricane Catarina (2004). Month Weather Rev 134:3029–3053

Nittrouer CA, Austin JA, Field ME, Kravitz JH, Syvitski JPM, Wiberg PL (2007) Writing a Rosetta stone: insights into continental-margin sedimentary processes and strata. In: Nittrouer CA, Austin JA, Field ME, Kravitz JH, Syvitski JPM, Wiberg PL (eds) Continental margin sedimentation: from sediment transport to sequence stratigraphy. Special Publication of the International Association of Sedimentologists, no 37. Blackwell, Malden, pp 1–48

Oberle FKJ, Hanebuth TJJ, Baasch B, Schwenk T (2014a) Volumetric budget calculation of sediment and carbon storage and export for a late Holocene mid-shelf mudbelt system (NW Iberia). Cont Shelf Res 76:12–24

Oberle FKJ, Storlazzi CD, Hanebuth TJJ (2014b) Wave-driven sediment mobilization on a storm-controlled continental shelf (Northwest Iberia). J Mar Syst 139:362–372

Palanques A, Plana F, Maldonado A (1990) Recent influence of man on the Ebro margin sedimentation system, northwestern Mediterranean Sea. Mar Geol 95:247–263

Palanques A, Masqué P, Puig P, Sanchez-Cabeza JA, Frignani M, Alvisi F (2008) Anthropogenic trace metals in the sedimentary record of the Llobregat continental shelf and adjacent Foix Submarine Canyon (northwestern Mediterranean). Mar Geol 248:213–227

Palinkas CM, Nittrouer CA, Walsh JP (2006) Inner-shelf sedimentation in the Gulf of Papua, New Guinea: a mud-rich shallow shelf setting. J Coast Res 22:760–772

Pezza AB, Simmonds I (2005) The first South Atlantic hurricane: unprecedent blocking, low shear and climate change. Geophys Res Lett. doi:10.1029/2005GL023390

Pilskaln CH, Churchill JH, Mayer LM (1998) Resuspension of sediment by bottom trawling in the Gulf of Maine and potential geochemical consequences. Conserv Biol 12:1223–1229

Riemann B, Hoffmann E (1991) Ecological consequences of dredging and bottom trawling in the Limfjord, Denmark. Mar Ecol Prog Ser 69:171–178

Rose L, Kuehl SA (2010) Recent sedimentation patterns and facies distribution on the Poverty Shelf, New Zealand. Mar Geol 270:160–174

Rúa A, Liebezeit G, Palacio-Baena J (2014) Mercury colonial footprint in Darién Gulf sediments, Colombia. Environ Earth Sci 71:1781–1789

Shi X, Liu Y, Chen Z, Wei J, Ge S, Wang K, Wang G, Yang S, Qiao S, Cai D, Cheng Z, Bu W, Yi H (2012) Origin, transport processes and distribution pattern of modern sediments in the Yellow Sea. In: Li MZ, Sherwood CR, Hill PR (eds) Sediments, morphology and sedimentary processes on continental shelves. Special Publication of the International Association of Sedimentologits, no 44. Blackwell, Malden, pp 321–344

Sommerfield CK, Wheatcroft RA (2007) Late Holocene sediment accumulation on the northern California shelf: oceanic, fluvial and anthropogenic influences. GSA Bull 119:1120–1134

Summerfield CK, Nittrouer CA (1999) Modern accumulation rates and a sediment budget for the Eel shelf: a flood-dominated depositional environment. Mar Geol 154:227–241

Thrush SF, Dayton PK (2002) Disturbance to marine benthic habitats by trawling and dredging: implications for marine biodiversity. Annu Rev Ecol Syst 33:449–473

Torres RJ, Abessa DMS, Santos FC, Maranho LA, Davanso MB, Nascimento MRL, Mozeto AA (2009) Effects of dredging operations on sediment quality: contaminant mobilization in dredged sediments from the Port of Santos, SP, Brazil. J Soils Sediment 9:420–432

Traykovski P, Geyer WR, Irish JD, Lynch JF (2000) The role of wave-induced density-driven fluid mudflows for cross-shelf transport on the Eel River continental shelf. Cont Shelf Res 20:2113–2140

USEPA (2008) Method 3050b. http://www.epa.gov/osw/hazard/test methods/sw846/pdfs/3050b.pdf. Accessed 30 Nov 2013

Vitorino J, Oliveira A, Jouanneau JM, Drago T (2002) Winter dynamics on the northern Portuguese shelf. Part 2: bottom boundary layers and sediment dispersal. Prog Oceanogr 52:155–170

Walsh JP, Nittrouer CA (2009) Understanding fine-grained river-sediment dispersal on continental margins. Mar Geol 263:34–45

Warnken KW, Gill GA, Dellapenna TM, Lehman RD, Harper DE, Allison MA (2003) The effects of shrimp trawling on sediment oxygen consumption and the fluxes of trace metals and nutrients from estuarine sediments. Estuar Coast Shelf Sci 57:25–42

Hanebuth TJJ, Lantzsch H, Nizou J (2015) Mud depocenters on continental shelves—appearance, initiation times, growth dynamics and stratigraphic relevance. Geo-Mar Lett. doi: 10. 1007/s00367-015-0422-6

Zembruscki SG (1979) Geomorfologia da margem continental sul brasileira e das bacias oceânicas adjacentes. In: Chaves HAF (ed) Geomorfologia da margem continental brasileira e áreas oceânicas adjacentes. REMAC Project Series. Petrobrás, Rio de Janeiro, pp 7–26

FIGURE CAPTIONS:

Figure. 1 Location of the sampling stations on the inner to middle shelf: surface samples (dots), box cores (black squares). The dashed line indicates the position of the chirp profile shown in Fig. 2. In the detailed map, diamonds indicate sediment cores from the Santos Estuarine Complex and crosses indicate surface samples from Santos Bay. For the location of the samples located in Santos Bay and Estuarine Complex see Martins et al. 2007, 2008, 2010

Figure. 2 Chirp profile across the shelf adjacent to the SECB showing the coastal and mid-shelf mudbelts (from the NAPGEOSEDEX cruise in 2013)

Figure 3 a. Box plot of Pb, Cu, and Zn in the sediments of the three local compartments analysed in this study. **b** Box plot of PAHs and aliphatic hydrocarbon concentrations in the three local compartments analysed.

Figure 4. Bathymetrical dependence of heavy metal concentrations (dots) and organic compounds (crosses)in the surface sediments of Santos Bay and the adjacent shelf

Figure 5. Geographical distribution of a Pb (mg kg -1) and b Zn (mg kg -1) in the surface sediments of the continental shelf.

Figure 6. Geographical distribution of a ΣPAH (ng kg -1) and b ΣAliphatic (µgkg -1) in the surface sediments of the continental shelf.

Figure 7. Concentration of Aliphatic (dots) and PAHs (crosses) along the sedimentary column of the three box cores #12 (left), #9 (centre), and #4 (right). Box core #9 was collected from the coastal mudbelt and the other two from the mid-shelf mudbelt

Figure 1

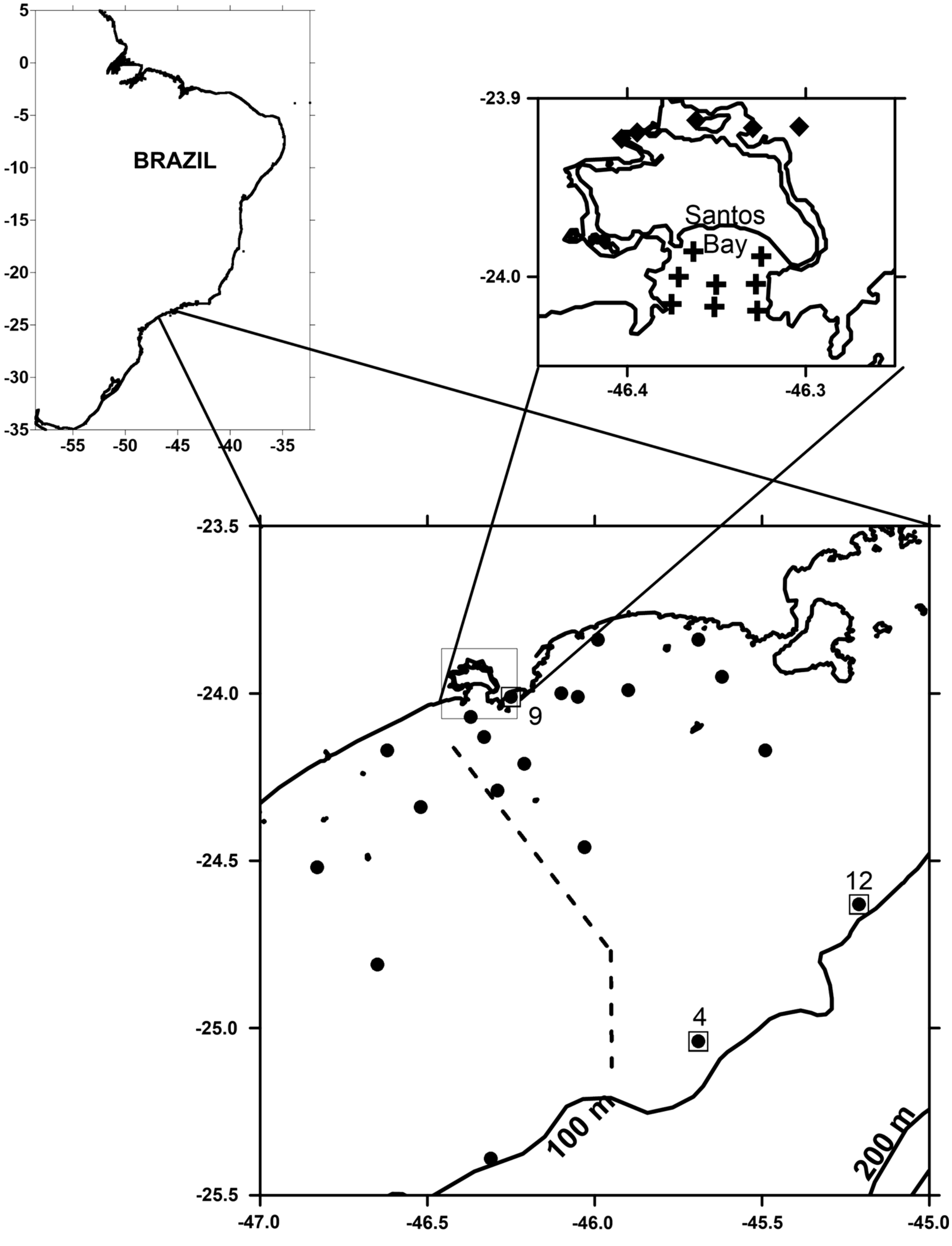
BRAZIL
5
0
-5
-10
-15
-20
-25
-30
-35
-55
-50
-45
-40
-35
Santos
Bay
-23.9
-24.0
-46.4
-46.3
-23.5
-24.0
-24.5
-25.0
-25.5
-47.0
-46.5
-46.0
-45.5
-45.0
9
12
4
100 m
200 m

Figure 2

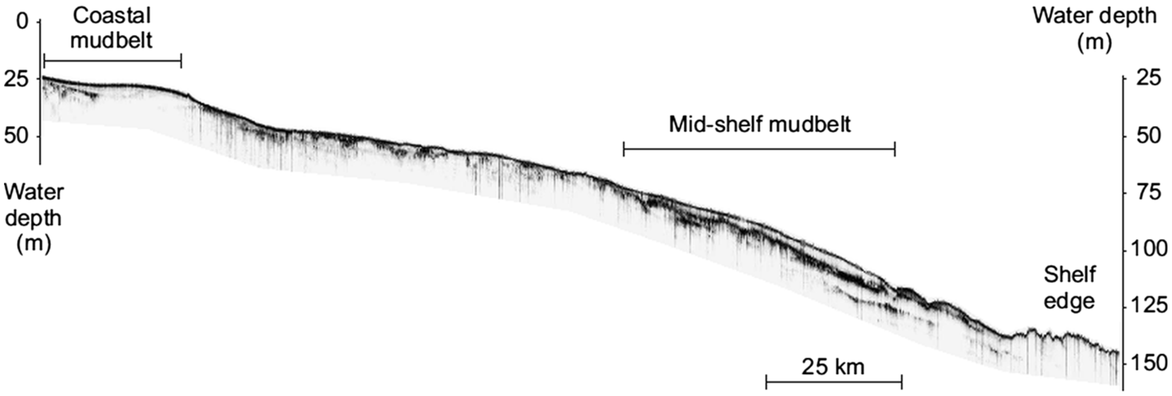
0
Coastal mudbelt
25
50
Water depth (m)
Mid-shelf mudbelt
Water depth (m)
25
50
75
100
125
150
Shelf edge
25 km

Figure 3

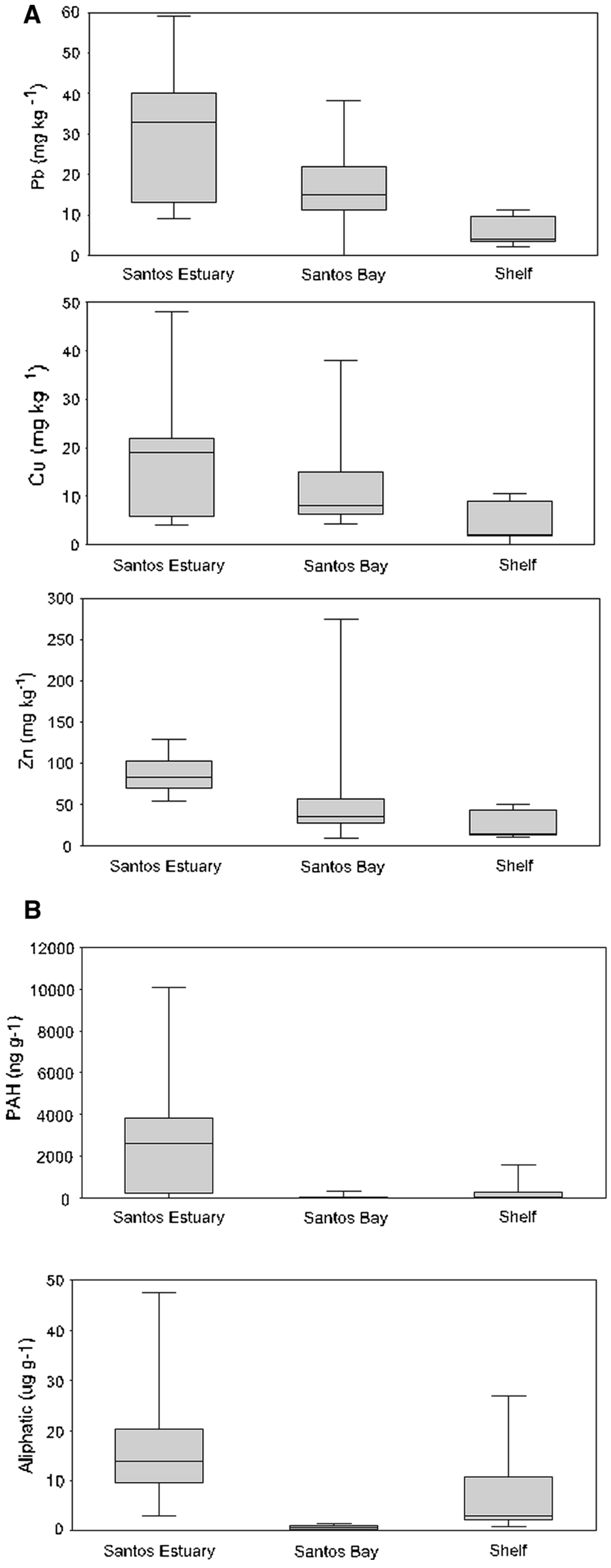
A
Pb (mg kg-1)
0
10
20
30
40
50
60
Santos Estuary
Santos Bay
Shelf
Cu (mg kg-1)
0
10
20
30
40
50
Santos Estuary
Santos Bay
Shelf
Zn (mg kg-1)
0
50
100
150
200
250
300
Santos Estuary
Santos Bay
Shelf
B
PAH (ng g-1)
0
2000
4000
6000
8000
10000
12000
Santos Estuary
Santos Bay
Shelf
Aliphatic (ug g-1)
0
10
20
30
40
50
Santos Estuary
Santos Bay
Shelf

Figure 4

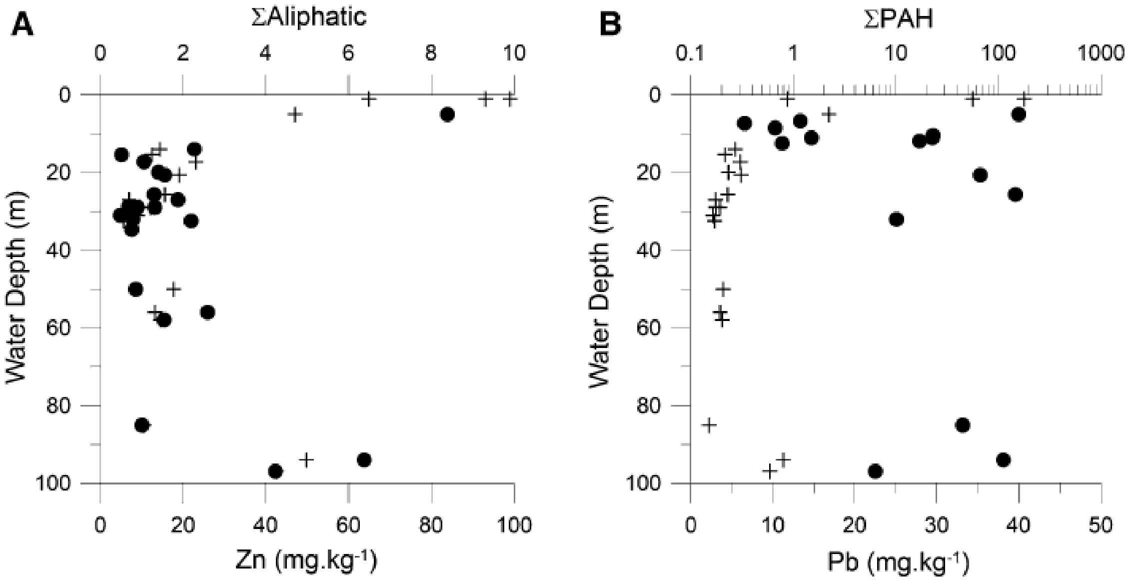
A
ΣAliphatic
0
2
4
6
8
10
Water Depth (m)
0
20
40
60
80
100
0
20
40
60
80
100
Zn (mg.kg-1)
B
ΣPAH
0.1
1
10
100
1000
Water Depth (m)
0
20
40
60
80
100
0
10
20
30
40
50
Pb (mg.kg-1)

Figure 5

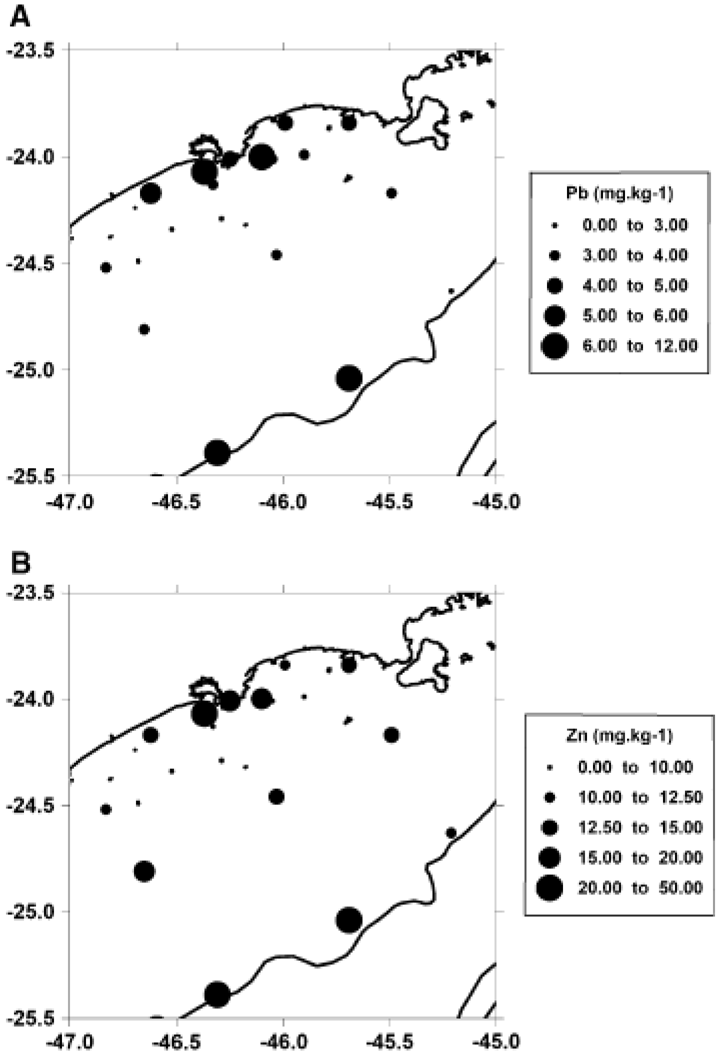
A
-23.5
-24.0
-24.5
-25.0
-25.5
-47.0
-46.5
-46.0
-45.5
-45.0
Pb (mg.kg-1)
0.00 to 3.00
3.00 to 4.00
4.00 to 5.00
5.00 to 6.00
6.00 to 12.00
B
-23.5
-24.0
-24.5
-25.0
-25.5
-47.0
-46.5
-46.0
-45.5
-45.0
Zn (mg.kg-1)
0.00 to 10.00
10.00 to 12.50
12.50 to 15.00
15.00 to 20.00
20.00 to 50.00

Figure 6

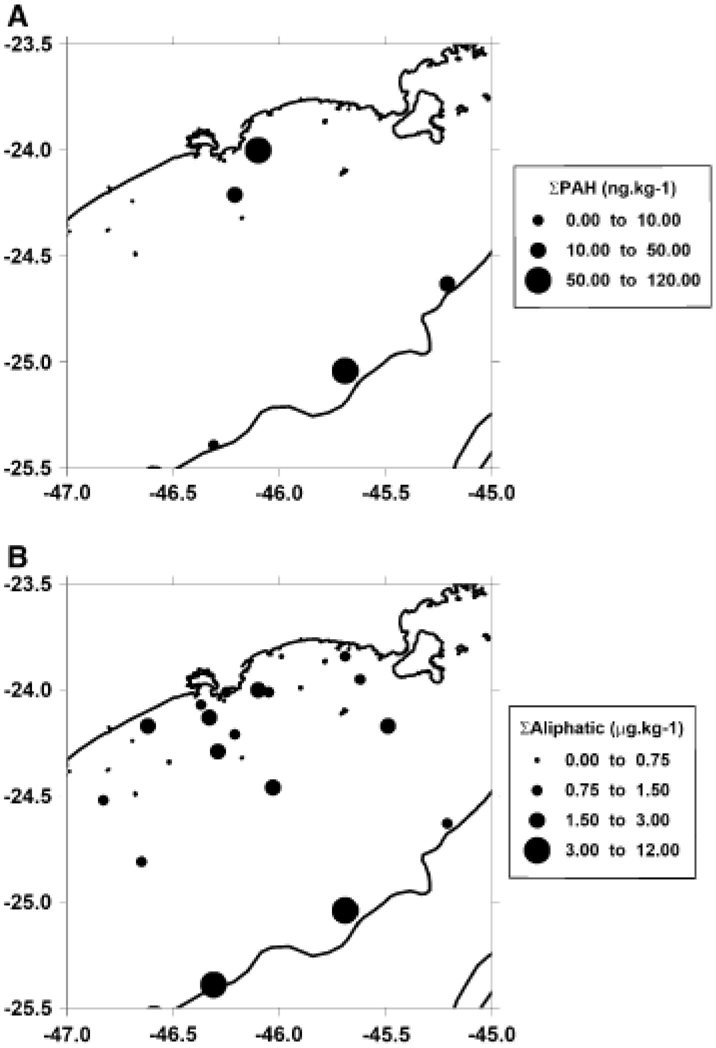
A
-23.5
-24.0
-24.5
-25.0
-25.5
-47.0
-46.5
-46.0
-45.5
-45.0
ΣPAH (ng.kg-1)
● 0.00 to 10.00
● 10.00 to 50.00
● 50.00 to 120.00
B
-23.5
-24.0
-24.5
-25.0
-25.5
-47.0
-46.5
-46.0
-45.5
-45.0
ΣAliphatic (μg.kg-1)
● 0.00 to 0.75
● 0.75 to 1.50
● 1.50 to 3.00
● 3.00 to 12.00

Figure 7

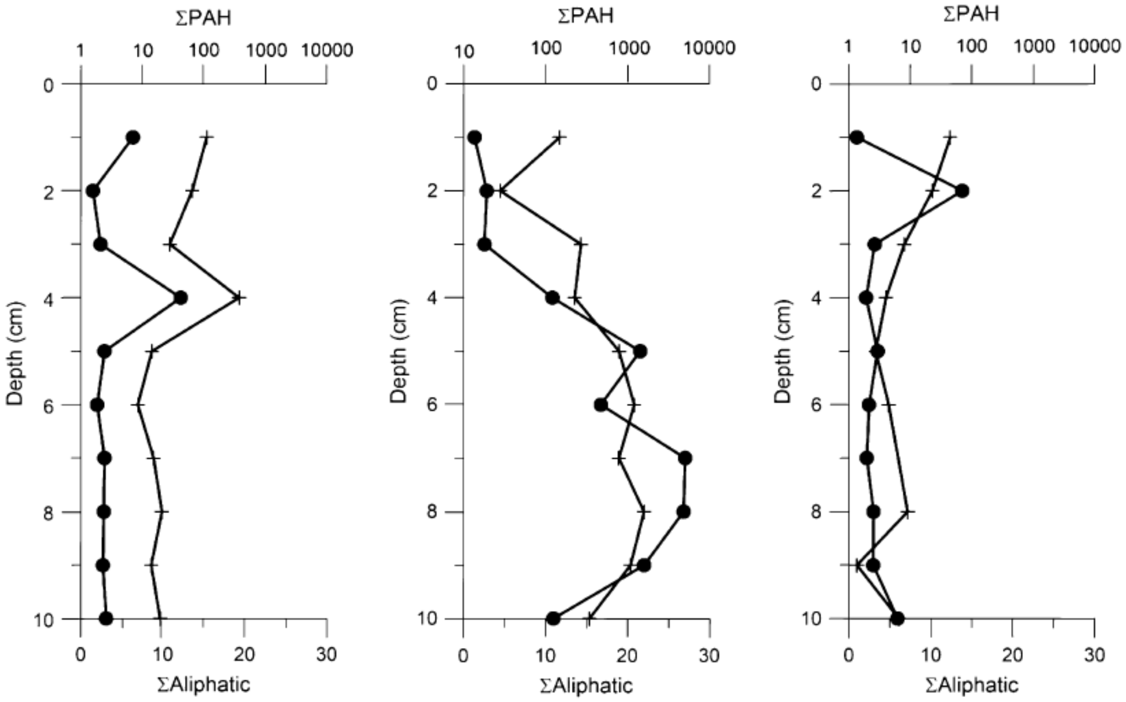
ΣPAH
1
10
100
1000
10000
0
2
4
6
8
10
Depth (cm)
0
10
20
30
ΣAliphatic
ΣPAH
10
100
1000
10000
0
2
4
6
8
10
Depth (cm)
0
10
20
30
ΣAliphatic
ΣPAH
1
10
100
1000
10000
0
2
4
6
8
10
Depth (cm)
0
10
20
30
ΣAliphatic